ISSN: 2277-3754
ISO 9001:2008 Certified
International Journal of Engineering and Innovative Technology (IJEIT)
Volume 4, Issue 10, April 2015

Modeling of TBM Tunnel Construction for the Greater Cairo Metro Line 3

S. Abdel Salam, Alaa Ata ,Osman Shaalan, Nadia Hammad
Department of Structural Engineering, Faculty of engineering, Zagazig University, Zagazig,
National Authority for Tunnels, Cairo, Egypt

Abstract*— In this paper, the ground surface settlements due to construction of tunnels by slurry shield tunnel boring Machine are predicted. The construction stages and parameters such as excavation, face and grouting pressures, jacking forces, etc. are simulated in a three dimensional finite elements analysis utilizing MIDAS software. The main objective is to simulate the conditions of a section along the route of the Greater Metro Line 3 Phase 1 and to compare the results with the actual settlement monitored during construction of the Project. The results of the maximum ground surface settlement show that numerical results are about 3.5 times the actual measured values. Results from sensitivity analyses for all parameters show that both the face and grout pressures are the most influencing parameters. Changing the values of face pressure results in considerable change in the values of the surface settlement as compared to changing the grout pressure. However, it is confirmed that a small change in the grout pressure results in greater changes in settlements as compared with a similar order of changes in face pressure.

***Index Terms*—face pressure, grout, TBM, tunneling slurry shield.**

I. INTRODUCTION

Construction of tunnels in soft grounds induces generally soil movement, which could seriously affect the stability and integrity of adjacent structures [1]. Because of its efficiency and safety, shield tunneling is one of the most popular tunneling methods for the construction of subway tunnels in soft soil ground [2]. Tunneling is a complex construction operation to undertake in the meantime considerable effort is required to predict the effects of tunnel construction, particularly in urban areas [3]. Analysis of the impact of the tunnel construction using TBM on the soil movement requires the solution of an elaborate 3D non-linear soil–structure interaction problem. Furthermore, shield tunneling usually adopts staged construction and supporting techniques, consequently, the responses such as soil displacements and lining forces induced by the construction will be different at different stages. Hence, it becomes very important to take into account the actual construction process in the shield tunneling analysis [2]. The numerical methods of structural analysis provide a powerful tool to simulate the different construction phases in geotechnical works. During the last forty years a significant development and advances in the application of the numerical methods have been achieved. In this paper a three-dimensional finite element model capable of representing the main tunnel construction aspects is presented. All details of the 3D FEM model are presented. The data used in this paper is based on actual and monitored parameters during the construction of Cairo Metro Line 3, Phase 1 where slurry shield boring machine was used.

II. 3D-FEM MODEL

The purpose of the numerical mechanized tunneling model is to take into consideration the large number of processes that take place during tunnel excavation and construction. The 3D finite element model consists of various components such as the soil layers, soil parameters, the tunneling machine, the hydraulic jacks, the tunnel lining and the tail void grout. All these parameters are calculated and simulated in the 3D FEM model.

A. Model Dimensions and soil Parameters

The tunnel model adopted here is based on the actual design documents of Phase 1 in Line 3 of the Cairo Metro. The construction of this Phase began in 2007 and was opened to operation in 2011. The boundaries of the model were selected to be faraway enough in order not to influence the results of the analysis. The mesh dimensions were selected following recommendations by Meissner (1996) [4], where (4-5)D from the tunnel center line to the vertical mesh boundaries and (2-3)D from the tunnel center point to the bottom boundary. Fig 1 shows the selected dimensions for 3D FEM model.

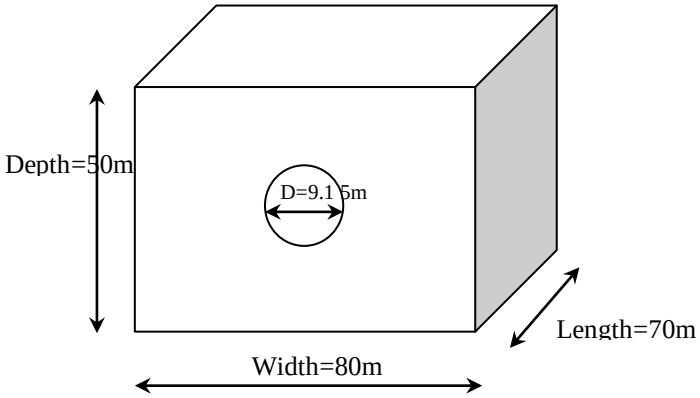

Fig 1 Dimensions selected for 3D FEM model

ISSN: 2277-3754
ISO 9001:2008 Certified
International Journal of Engineering and Innovative Technology (IJEIT)
Volume 4, Issue 10, April 2015

In Cairo Metro Line 3 Phase 1, there are many sections where the tunnel is located at different depths below the ground surface. The tunnel section at KP=18.75 is selected for verification of the numerical model in this study as it represents the shallowest and the most critical section. Figure 2 shows the soil layers at this section and their levels [5]. Table 1 summaries the soil parameters used in the 3D FEM model and Table 2 gives the levels of the soil layers and the ground water [5]. Mohr-Coulomb model is selected to model the soil in the present analysis.. The Mohr-Coulomb model requires five parameters; namely Young's modulus, Poisson's ratio, cohesion, friction angle, and dilatancy angle.

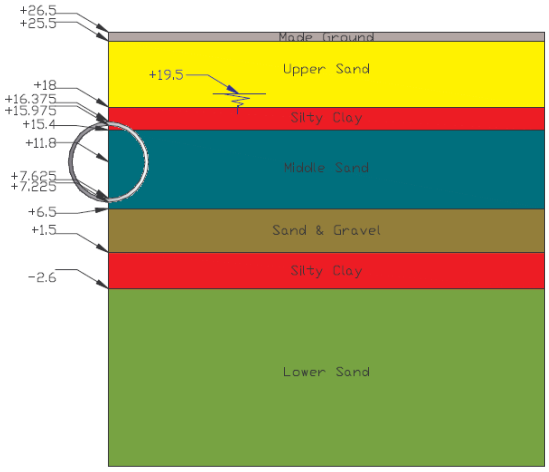

Fig 2 Soil layers at section at KP=18.75 [5]

Layer Id.	Soil unit weight (kN/m^3)	Case of during construction		Case of Final condition	
		Shear strength parameters	Deformation parameters	Shear strength parameters	Deformation parameters
Made Ground	17.0	c = 0.0 Φ = 27°	E = 4 MPa ν = 0.3	c = 0.0 Φ = 27°	E = 4 Mpa ν = 0.3
Upper Sand	19.5	c = 0.0 Φ = 36°	E = 40 Mpa ν = 0.3	c = 0.0 Φ = 36°	E = 40 Mpa ν = 0.3
Middle Sand	19.5	c = 0.0 Φ = 38°	E = 70 Mpa ν = 0.3	c = 0.0 Φ = 38°	E = 70 Mpa ν = 0.3
Lower Sand	19.5	c = 0.0 Φ = 38°	E = 120 Mpa ν = 0.3	c = 0.0 Φ = 38°	E = 120 Mpa ν = 0.3
Silty Clay	19.5	c_u = 90 kPa $\Phi_u = 0^0$	E_u = 22 Mpa ν = 0.49	c_d = 0 kPa $\Phi_d = 29^0$	E_d = 20 Mpa ν = 0.35
Sand & Gravel	20.0	c = 0.0 Φ = 41°	E = 100 Mpa ν = 0.3	c = 0.0 Φ = 41°	E = 100 Mpa ν = 0.3

Table 1 Soil Parameters for soil layers at section at KP=18.75 [5]

cml 18.75	
Layer Id.	Top level [m]
Made Ground	26.5
Upper Sand	25.5
Silty Clay	18
Middle Sand	15.4
Sand & Gravel	6.5
Silty Clay	1.5
Lower Sand	-2.6
Water Level	19.5
Tunnel Axis Level	11.8

Table 2 Levels of the soil layers, the tunnel And the ground water table [5]

B. Structural Elements Properties

In the model the TBM (tunnel boring machine) is modeled as plate elements and assumed as 10.5 m long instead of 11 m in order to fit seven standard slices in the analysis. The segmental tunnel lining is also modeled as plate elements. Table 3 shows the parameters of the shield TBM machine [5].

Table 3 Structural properties of the shield [5]

Shield Parameters	
Overcut diameter (m)	9.15
Shield tail diameter, extrados (m)	9.15
Thickness (mm)	40
Modulus of elasticity (GPa)	205
Length (m)	10.5
Approx. weight (Tonne)	870

The lining is installed when the annulus grout becomes hardened. The bending stiffness of the lining is based on the reduced moment of inertia proposed by Muir Wood (1975) [6] for the jointed lining. Bored tunnel lining parameters are as follows:

- Internal diameter 8.35 m
- Lining thickness 0.40 m
- Ring mean length 1.50 m
- Specific self-weight: 25 kN/m^3
- Long term modulus of elasticity : E_c = 15.160 MPa
- Poisson's ratio: 0.20

As the thickness of segments is not constant due to the longitudinal joints of the segments constituting the rings of the tunnel, a reduction in flexural stiffness of the lining should be taken into consideration, based on Muir Wood [6]. The calculation of the reduced stiffness of the lining is as follows:

- Typical segment section: 1.5 m x 0.4 m
- Typical segment inertia(I Typical):
- I Typical = 1.5 x $(0.4)^3/12$=0.008 m^4
- Longitudinal contact section: 1.35 m x 0.24 m
- Longitudinal contact inertia($I_{Contact}$t):
- $I_{Contact}$ = 1.35 x $(0.24)^3/12$=0.00156 m^4
- Equivalent number of standard segments(N): N= 7
- Muir Wood inertia reduction ratio (mw):
  mw= $I_{Contact}/I_{Typical}$ + (4/N)2= (.00156/0.008)= 0.521
- Equivalent lining section thickness(th_{equiv}):
  th_{equiv}= mv1/3 x $th_{typical}$ =(0.521)1/3 x 0.4= 0.32 m
  Revise and clarify what is mv.

Thus after the calculation of the Muir Wood reduction ratio and the equivalent lining section thickness, the tunnel lining is modeled as a continuous with a reduced thickness of 0.32 m.

C. Loads

During the construction of the bored tunnel there are several loads affecting the construction process, such as the

ISSN: 2277-3754
ISO 9001:2008 Certified
International Journal of Engineering and Innovative Technology (IJEIT)
Volume 4, Issue 10, April 2015

face pressure which keeps the excavation stable. The face pressure is calculated as equal to the hydrostatic pressure and is acting in the horizontal direction. The face pressure, needed to ensure the stability of the tunnel face and to minimize the surface settlement, can be divided into 2 parts [5]:

- The first is equal to the existing pore water pressure at the section location and its role is to equilibrate the existing water pressure at the tunnel level.
- The second is the part of the pressure in excess to the ground water pressure which is used to ensure the face stability and to govern the soil deformation and so the settlements.

The retaining pressure must be everywhere greater than the hydrostatic pressure, as illustrated by Figure 3.

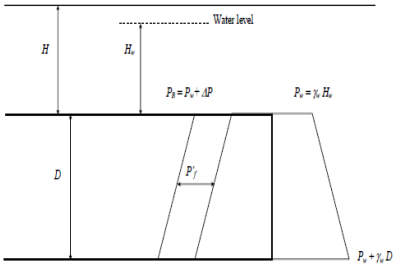

Fig 3 The calculation of face pressure [5]

Where,

- P_B is the slurry pressure at the tunnel crown..
- P_W is the hydrostatic pressure at the tunnel crown..
- If the required pressure is ΔP, then [5]:

$$P_B \geq P_W + \Delta P \quad (1)$$

$$P_w = \gamma_w \times H_w \quad (2)$$

Where γ_w is the unit weight of water and H_w is the height of the water head above the tunnel crown (usually, ΔP≡ 10 kPa [5]). The retaining pressure needed for the adopted 3D FEM model is calculated to be equal to 250 kN/m^2.

Grouting under pressure is required to fill the gap between lining and the soil due to the over cutting. The grout pressure must be greater than the external hydrostatic pressure acting on the lining at the time of grouting. In large diameter tunnels the difference in hydrostatic pressure between the crown and the invert can be considerable. However, it must be noted that excessive volume of grout and/or pressure may cause damage to the lining, or cause ground heave, which could affect surface or subsurface structures and services [7]. In general, the backfill grouting pressure is set to be in the range of 50-100 KN/m^2 higher than that of the slurry pressure [8]. As the calculated face pressure is 250 KN/m^2, then the grouting pressure will be considered as 350 KN/m^2. This load will be applied around the tunnel in the vertical direction. The grout injected into the tail void is, for this analysis, assumed to be in liquid state over the three lining segments located just behind the shield, i.e., a distance of 10.5 to 15 m. After a distance of 15 m, the grout is assumed to be hardened and is activated in the model. The hard grout material should be at least as rigid as the surrounding ground and transmits the efforts of the ground solid mass the lining [9]. Table 4 gives the properties of the hard grout as included in the 3D FEM model.

Hard Grout Parameters	
Thickness (mm)	15
Modulus of elasticity (GPa)	10
Poisson's ratio	0.3
Unit weight (KN/m^2)	23

Table 4 the structural properties of the shield [9]

During the shield tunneling operation, the shield is driven forward by applying mechanical jacking forces behind the machine tail and excavation the soil in front of the machine with the cutting face. Jacks installed in the shield push the shield away from the installed lining into the soil. After each sequential tunnel advance of one segment length, the jacks are released, giving space for a new lining ring to be built. The frictional force denoted $F_{Friction}$ is related to the force exerted on the face $F_{Faceand}$ the jacking force F_{Jack} by the equation, [10]:

$$F_{Friction} = F_{Jack} - F_{Face} = \sigma_{jack} * A_{lining} - \sigma_{Face} * A_{Face} \quad (3)$$

Where:

σ_{Jack}: Average jack pressure

A_{Lining}: Cross- section area of the lining

σ_{Face} : Face pressure on the face

A_{Face}: Cross- section area of the face

The frictional force is given by [10]:

$$F_{Friction} = \mu * N_{Friction} \quad (4)$$

Where:

μ: Coefficient of sliding friction between the soil and the shield

$N_{Friction}$: Normal force acting on the shield.

Empirical values of μare reported for sand, μ is between 0.3 and 0.6; for clay, μranges from 0.2 to 004. In this model the tunnel exists in the middle sand layer, so the value of the coefficient of sliding friction is chosen 0.4[11].

The normal force acting on the tail skin is obtained by integrating the normal stress acting on the external surface of the shield [12] by,

$$N_{Friction} = L.D_e.\frac{\pi}{2}\left[\sigma_{Ev} + \frac{\gamma.D_e}{2} + K_0\left(\sigma_{Ev} + \frac{\gamma.D_e}{2}\right)\right] \quad (5)$$

Where:

L: Length of the shield

D_e: Outer diameter of shield

γ: Total unit weight of soil

K_0: Coefficient of earth pressure at rest

σ_{Ev}: Vertical stress at the tunnel crown.

The vertical stress at the tunnel crown is often computed using the arching model [13],

$$\sigma_{Ev} = \frac{b\left(\gamma - \frac{2.c}{b}\right)}{2.K_0.\tan\emptyset}\left[1 - e^{-2.K_0\tan\emptyset\left(\frac{h}{b}\right)}\right] \quad (6)$$

Where:

ISSN: 2277-3754
ISO 9001:2008 Certified
International Journal of Engineering and Innovative Technology (IJEIT)
Volume 4, Issue 10, April 2015

c: Cohesion of soil
h: Height of cover at tunnel crown
φ: The angle of friction of soil

$$b = D_e\left[1 + 2.tan\left(45^0 - \frac{\emptyset}{2}\right)\right] \quad (7)$$

From the above mentioned equations (4, 5, 6, 7), the value of the jacking force can be calculated. The jacking forces will be applied at the tail of the shield on the lining.

The live loads applied on top of ground are considered as uniformly distributed loads of 12 kN/m^2. The loads of the nearby building are also considered in the calculation of the surface loads as they affect on the surface settlement. The following assumptions are made:

Nearby buildings founded on strip footings = 40 to 60 kN per linear meter per floor [14], therefore the building surface load Q is calculated as,

Q = number of floor × Q_{floor} (in kN /m) (8)

The floor equivalent load (self-weight + average floor live load) is taken as 12 kPa per floor [14].

In this case study the building loads is 48kPa [7].

D. Construction stage Process

Construction stage analysis consists of multiple stages and loading/boundary conditions, as well as elements that can be added or removed at each stage. This loading/boundary or element change is applied at the start of each stage [15]. In the 3D EFM model; there are 46 construction stages in addition the initial stage which simulates the initial stress in the model before excavating the tunnel. Stages from 1 to 7 simulate the progress of the shield inside the soil. There three stages after that to simulate the soft grout pressure after the tail skin of the shield. The rest of the stages are to simulate the erection of the tunnel lining and the hard grout. The construction stages can be summarized as follows.

Stage 0: Initial ground stress

Stages 1 to 7: shield progress, application of the face pressure load, erecting the first ring of the lining inside the shield and applying the jacking force on it.

Stage 8 to 10: erecting three rings behind the shield and applying the grout pressure simulating to the soft grout behind the tail skin of the shield.

Stage 11: erecting the fourth ring and the soft grout is considered hardened

Stage 12 to 45: repeating stages from 1 to 11.

Figure 4 shows the above summarized excavation process at the end of the 46 stages while table 5 shows the activation and the re-activation of the structural elements during construction stages, from stage 1 stage 11, as they are done in the Midas GTX NX Software and the 3D FEM model.

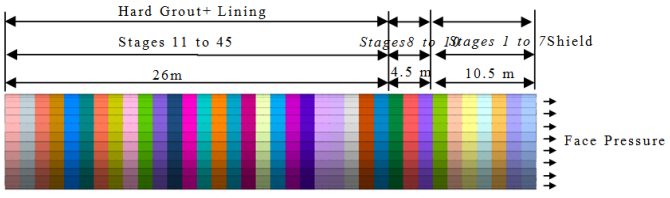

Fig 4 Construction stages as extracted from Midas software

Set Name Prefix	S1	S2	S3	S4	S5	S6	S7	S8	S9	S 10
Shield	A: 1	A: 2	A: 3	A: 4	A: 5	A: 6	A: 7	A: 8 R: 1	A: 9 R: 2	A: 10 R: 3
Segment							A: 1	A: 2	A: 3	A: 4
Face pressure	A: 1	A: 2 R: 1	A: 3 R: 2	A: 4 R: 3	A: 5 R: 4	A: 6 R: 5	A: 7 R: 6	A: 8 R: 7	A: 9 R: 8	A: 10 R: 9
Grout force								A: 1	A: 2	A: 3 R: 1
Jacking force							A: 1	A: 2 R: 1	A: 3 R: 2	A: 4 R: 3
Hard grout										A: 1

Where:S: stage numberA: ActivatedR: Re-activated

Table 4 Activation and re-activation during construction stages

III. RESULTS

Figure 5 shows the vertical settlements at the crown and the invert of the tunnel during different stages of the tunnel's construction. It can be noticed that at all stages there is a settlement at the crown of the tunnel while the displacement at the invert of the tunnel is heave. Figure 6 shows that the settlement is increasing while the TBM machine is advancing which is compatible with the well-known pattern of the TBM settlement; this is also illustrated in Figure 7.

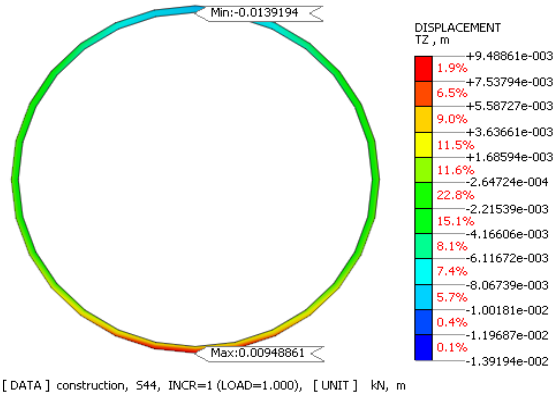

Fig 5 Settlement at the tunnel crown and invert at stage 44

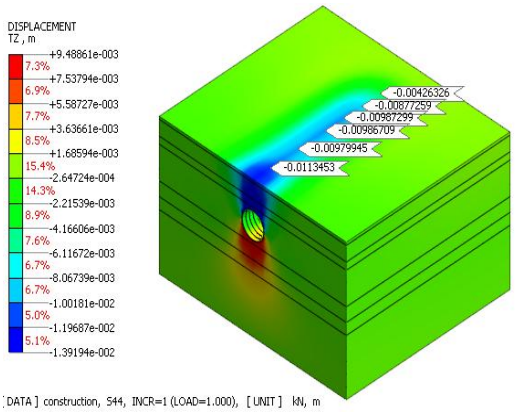

Fig 6 Ground surface settlement at stage 44

Figure 7 shows a comparison between the ground settlement troughs for different construction stages. It can be observed that the maximum settlement is always at the center of the tunnel at 40 m on the Y-axis. A comparison between the results gotten from the Midas GTX NX 3D FEM and the 2D FEM done in Cairo Metro Line 3 Phase 1 design

ISSN: 2277-3754
ISO 9001:2008 Certified
International Journal of Engineering and Innovative Technology (IJEIT)
Volume 4, Issue 10, April 2015

documents, show that the values of the settlement in the 3D FEM model is relatively small compared with the 2D EFM, refer to Figures 8 and 9. Figure 8 shows that the maximum settlement is 14.8 mm, while in the 3D model it is only 13.9 mm. According to the official monitoring report of Cairo Metro Line 3 Phase 1, the actual settlement is only 4 mm, and it was recorded after the shield machine has passed the monitoring point by a distance of 860 m. This settlement value is very small compared with the calculated surface settlement from the 3D FEM which means that the theoretical analysis includes much conservative assumptions.

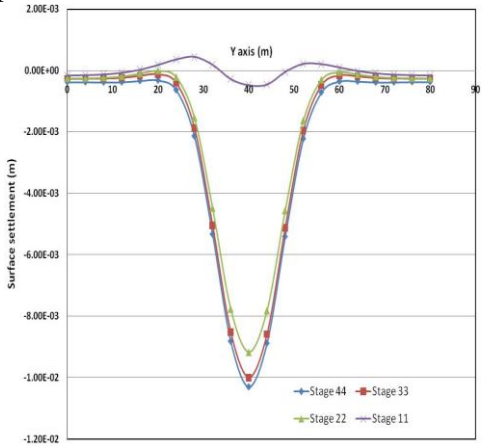

Fig 7 Comparison between settlement troughs at different construction stages

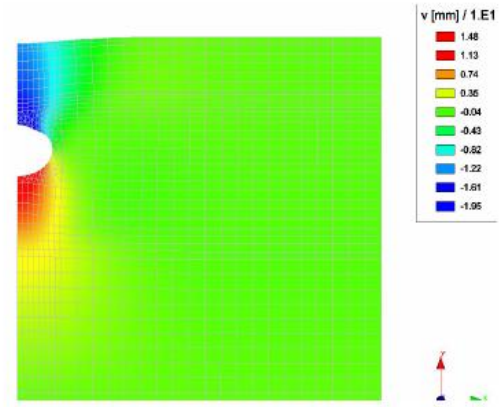

Fig 8 Values of the settlement according to SECAR LCPC 2D FEM model [7]

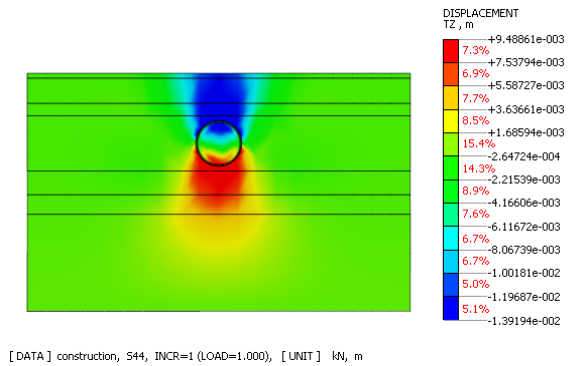

Fig 9 Values of the settlement according to Midas GTX NX 3D FEM model

IV. SENSITIVITY STUDY

To have a better understanding of the effects of both the face pressure and the grout pressure, sensitivity analyses were performed by applying different levels of face and grout pressures, separately. Values of face pressures of 200, 250, 300, 350 kN/m^2 were applied to investigate the effect of the face pressure. The values of the surface settlements at different values of face pressure are shown in Figures 10, 11 and 12. Figure 10 present the surface settlements at face of the TBM machine, while Figure 11 presents the surface settlement at the tail of the TBM machine. The longitudinal surface settlement is shown in Figure 12.

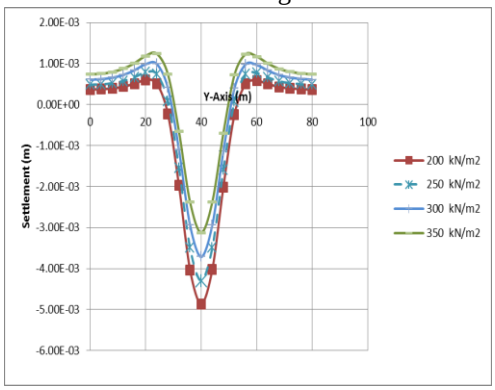

Fig 10 The surface settlements at different values of face pressure at the face of the TBM machine

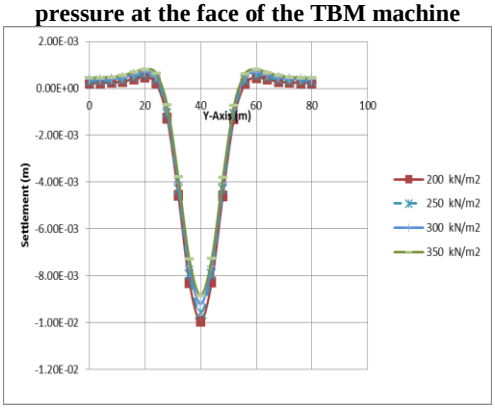

Fig 11 The surface settlements at different values of face pressure at the tail of the TBM machine

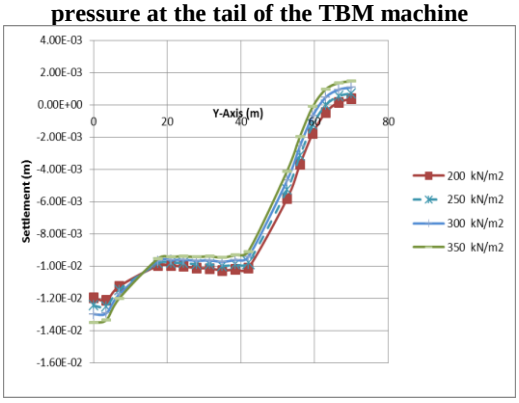

Fig 12 the longitudinal surface settlements at different values of face pressure

It can be seen from the three figures that increasing the face pressure results in decreasing the value of the surface

ISSN: 2277-3754
ISO 9001:2008 Certified
International Journal of Engineering and Innovative Technology (IJEIT)
Volume 4, Issue 10, April 2015

settlement. It can also be seen that the surface settlement at the face of the TBM machine is relatively small compared with the surface pressure at the tail of the TBM machine. Figure 12 shows increase in the surface settlement with the advancement of the TBM machine. Figures 13, 14 and 15 illustrate the influence of the grout pressure on the surface settlement. It can be observed that increasing the grout pressure also results in decreasing settlements, however, values of the settlements are more sensitive to changes in the face pressure as compared to changes in grout pressure. Comparing between the values of the settlements resulting from changing the face pressure and the grout pressure, it can be noticed that settlement values from the grout pressure is remarkably bigger than those from the face pressure.

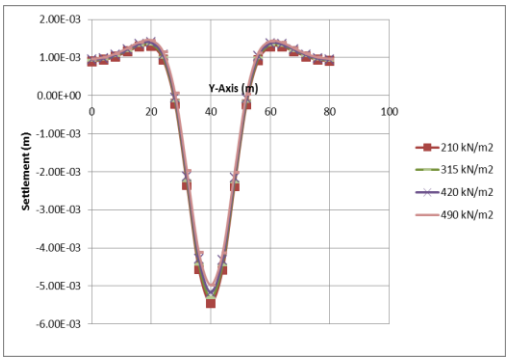

Fig 13 Surface settlements at different values of grout pressure at the face of the TBM machine

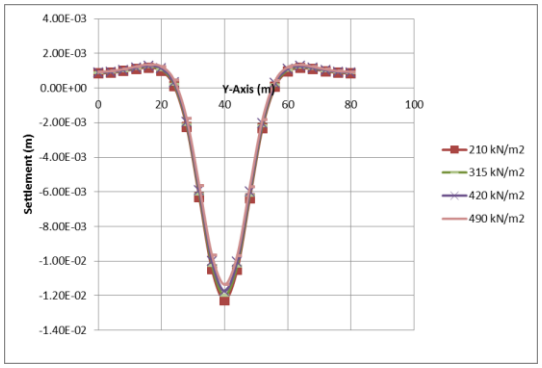

Fig 14 Surface settlements at different values of grout pressure at the tail of the TBM machine

V. CONCLUSIONS

A three dimensional finite element simulation model for tunneling excavation is presented. All the parameters affecting the excavation process such as face pressure, grout pressure, jacking force…etc., are simulated. The construction stages are also simulated using Midas GTX NX software. A case study from Cairo Metro Line 3 Phase 1 is applied as case study. The results are compared with the calculated values in the Project design documents as well as the actual records from the Project site. It can be concluded that the theatrical methods of calculation of the surface settlement are very conservative. A sensitivity analysis is performed to study the Effect of both the face and grout pressures on the ground surface settlement. It can be concluded that changing the values of face pressure results in considerable change in the values of the surface settlement compared with changing grout pressure.

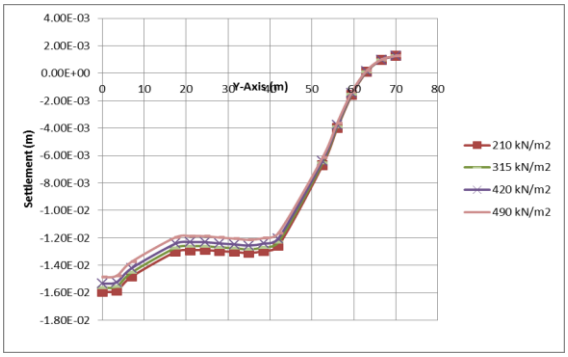

Fig 15 Longitudinal surface settlements at different values of grout pressure

VI. FUTURE ENHANCEMENT

The future work includes studying all parameters that might affect on the surface ground settlement. The parameters include the jacking force of the TBM, the soil parameters, the ground water table as well as the surface surcharge load.

REFERENCES

[1] H. Mroueh and I. Shahrour, "A simplified 3D model for tunnel construction using tunnel boring machines", Tunneling and Underground Space Technology, pp. 38–45, January 2007.

[2] W. Q. Ding, Z. Q. Yue and L. G. Tham, H. H. Zhu, C. F. Lee and T. Hashimoto, "International Journal for Numerical and Analytical Methods in Geomechanics", pp. 28:57–91, August 2004.

[3] D.K. Koungelis and C.E. Augarde, "Parameterized mesh generation for finite element analysis of Tunneling", Computers and Geomechanics, pp.1-41, November 2008.

[4] H. Meissner, "Numerik in der Geotechnik",der Deutschen Gesellschaft für Geotechnik, Issue 2, 1996.

[5] Cairo Metro Line 3 Phase 1 Design Documents, "401G2VTU000N001C", pp. 1-27, March 2008.

[6] A.M. Muir Wood, "The Circular Tunnel in Elastic Ground", Geotechnique 25 No. 1, pp. 115-127, 1975.

[7] ITA ITA-Working Group Research, "Guidelines for Design of Shield Tunnel Lining", pp. 1-49, November 1999.

[8] Standard Specifications for Tunneling, Shield Tunnels, Japan Society of Civil Engineers, 2006.

[9] T. Kasper and G. Meschke, " 3D finite element simulation model for TBM tunneling in soft ground", International Journal for Numerical and Analytical Methods in Geomechanics, 28(14),pp. 1441 – 1460, December 2004.

[10] J. D. Greenwood, "Three-Dimensional Analysis of Surface Settlement in Soft Ground Tunneling", Massachusetts Institute of Technology, pp. 54-56, June 2003.

ISSN: 2277-3754
ISO 9001:2008 Certified
International Journal of Engineering and Innovative Technology (IJEIT)
Volume 4, Issue 10, April 2015

[11] . Stein, K. Mollers and R. Bieleck, "Micro Tunneling Installation and Renewal of Norman-Size Supply and sewage Lines by Trenchless Construction method", ISBN 3-433-0120.6 Ernst& Sohn, Berlin, 1989.

[12] A. Pellet and R. Kastner, "Comparison of Micro Tunneling Jacking Force Theoretical Calculation and Experimental Data", In Proc. World Tunneling Congress, pp. 733-738, 1998.

[13] K. Terzaghi, "Theoretical Soil Mechanics", John Wiley & Sons, 1951.

[14] Cairo Metro Line 3 Phase 1 Design Documents, "403G2VTU000N001C", pp. 1-76, March 2008.

[15] GTSNX/MIDAS, (v.1.0.0) manual- Copyright Since1989 MIDAS Information Technology Co. Ltd, 2014.

AUTHOR'S PROFILE

First Author Sayed Abdel Salam is, Vice dean and Chairman of Structural Engineering Depart.,(Former), a Professor of Structural Engineering Faculty of Engineering, Zagazig University .

Second Author Alaa Ata is a professor of Geotechnical Engineering at the Department of Structural Engineering, and General Manager of the Credit Hour Programs at the Faculty of Eng., Zagazig University, Egypt. His research interests include: soil improvement, deep foundations, recycling of industrial wastes, and properties of calcareous sands.

Third Author Osman Shaalan Chairman of Structural Engineering Department and Professor of Structural Engineering, Faculty of Engineering, Zagazig University.

Forth Author Nadia Hammad is a general manager of technical research at National Authority for Tunnels, Cairo, Egypt. Her research interests include tunnel excavation and TBM performance during tunneling in soft grounds